Published in final edited form as:
J Periodontol. 2008 August ; 79(8): 1480–1490. doi:10.1902/jop.2008.070624.

Periostin Is Essential for the Integrity and Function of the Periodontal Ligament During Occlusal Loading in Mice

H.F. Rios[*,†], **D. Ma**[†,‡], **Y. Xie**[†,‡], **W.V. Giannobile**[*], **L.F. Bonewald**[†], **S.J. Conway**[§], and **J.Q. Feng**[†,‡]

[*] *Department of Periodontics and Oral Medicine, School of Dentistry, University of Michigan, Ann Arbor, MI*

[†] *Department of Oral Biology, School of Dentistry, University of Missouri–Kansas City, Kansas City, MO*

[‡] *Department of Biomedical Sciences, Baylor College of Dentistry, Dallas, TX*

[§] *Department of Pediatrics, Indiana University, Indianapolis, IN*

Abstract

Background—The ability of the periodontal ligament (PDL) to absorb and distribute forces is necessary for periodontal homeostasis. This adaptive response may be determined, in part, by a key molecule, periostin, which maintains the integrity of the PDL during occlusal function and inflammation. Periostin is primarily expressed in the PDL and is highly homologous to βig-H3 (transforming growth factor-beta [TGF-β] inducible gene). Cementum, alveolar bone, and the PDL of periostin-null mice dramatically deteriorate following tooth eruption. The purpose of this study was to determine the role of periostin in maintaining the functional integrity of the periodontium.

Methods—The periodontia from periostin-null mice were characterized followed by unloading the incisors. The effect of substrate stretching on periostin expression was evaluated using a murine PDL cell line. Real-time reverse transcription-polymerase chain reaction was used to quantify mRNA levels of periostin and TGF-β. TGF-β1 neutralizing antibodies were used to determine whether the effects of substrate stretching on periostin expression are mediated through TGF-β.

Results—Severe periodontal defects were observed in the periostin-null mice after tooth eruption. The removal of masticatory forces in periostin-null mice rescue the periodontal defects. Periostin expression was increased in strained PDL cells by 9.2-fold at 48 hours and was preceded by a transient increase in TGF-β mRNA in vitro. Elevation of periostin in response to mechanical stress was blocked by the addition of 2.5 ng/ml neutralizing antibody to TGF-β1, suggesting that mechanical strain activates TGF-β to have potential autocrine effects and to increase periostin expression.

Conclusion—Mechanical loading maintains sufficient periostin expression to ensure the integrity of the periodontium in response to occlusal load.

Keywords

Alveolar bone loss; animal study; cell adhesion molecule; periodontitis; periodontium

The structure and function of the periodontal tissues are intimately related to occlusal function. The periodontal ligament (PDL) is a functionally important tissue in tooth support,

Correspondence: Dr. Hector F. Rios, Department of Periodontics and Oral Medicine, School of Dentistry, University of Michigan, 1011 N. University, Ann Arbor, MI 48109-1078. Fax: 734/936-0374; e-mail: hrios@umich.edu.

The authors report no conflicts of interest related to this study.

proprioception, and regulation of the alveolar bone volume.[1] Current research[2,3] suggests that PDL cells respond directly to mechanical forces and adapt to the mechanical challenge by activation of mechanosensory signaling systems, cytoskeletal changes, and extracellular matrix organization.

Although there is a large body of evidence demonstrating the importance of the PDL for the load-related bone remodeling in periodontal homeostasis,[4-11] many of the molecular mediators of adaptive responses remain to be elucidated. In particular, there is a compelling need to identify molecules that are critical in the pathways regulating the structural characteristics and function of the PDL. Previously, we reported dramatic posteruption PDL defects that resulted from the in vivo deletion of periostin.[12] Periostin, a secreted disulfide-linked 90-kDa protein, was originally termed osteoblast-specific factor-2 (Osf-2) when first isolated from the mouse MC3T3-E1 osteoblastic cell line.[13] Because several other factors at the time were called Osf-2, the protein was renamed “periostin,” based on its localization in the periosteum and PDL, suggesting a potential role in bone and tooth formation and the maintenance of structure.[14] Periostin was reported to support MC3T3-E1 cell attachment and spreading and $\alpha_v\beta_3$ and $\alpha_v\beta_5$ integrin-dependent cell adhesion and cell motility.[14,15] Periostin's capacity to interact with cell membrane and extracellular matrix supports a role in the activation of the Akt/protein kinase B pathway to promote cellular survival.[16] It also was suggested that periostin is an important mediator of the biomechanical properties of fibrous connective tissues because it can regulate collagen I fibrillogenesis.[17] Wilde et al.[18] demonstrated that periostin mRNA was upregulated in compression sites compared to tension sites of the PDL after mechanical stress in the experimental tooth movement model. Later, it was shown that a transient decrease in periostin mRNA levels occurred during conditions of induced hypofunction,[19] which suggests that occlusal forces have a putative role in periostin expression in the PDL and that its expression might be functionally determined by the mechanically challenging environment. Periostin was shown to be regulated by TGF-β,[14] a multipotent factor known to regulate matrix production. TGF-β is activated when released from a large latent complex by factors such as low pH and proteases.[20] The latent TGF-β complex can also be activated by mechanical stretching.[21]

The purpose of this study was to investigate the importance of periostin in the function of the PDL. We hypothesized that periostin is regulated by mechanical stress and its expression is essential for the integrity and function of the PDL.

Materials and Methods

Mouse Maintenance and Husbandry

Periostin knock-out mice that were generated and described previously[12] were weaned at 3 weeks of age and fed distilled water and pellets.[‖] Mice were maintained under specific pathogen-free conditions with a 12-hour light/12-hour dark cycle. The animal use protocols were approved by the University of Missouri Kansas City Institutional Animal Care and Use Committee. Genotyping was determined by polymerase chain reaction (PCR) analysis of genomic DNA with primers p01: 5′-AGTGTGCAGATGTTTGCTTG-3′ and p02: 5′-ACGAAATACAGTTTGGTAATCC-3′ to detect the wild-type allele (~300 base pairs [bp]); and primers p01: 5′-AGTGTGCAGATGTTTGCTTG-3′ and primers p03: 5′-CAGCGCATCGCCTTCTATCG-3′ to detect the targeted allele (~700 bp).

[‖]NIH-31 Complete Mouse Diet, Denver, CO.

Radiography

Radiographs were used as a non-invasive means to measure changes in the periodontium. Radiographs were taken using a radiographic inspection unit with digital image–capture capabilities.[¶] Digitized images were analyzed using the analysis software to measure and evaluate PDL space, incisor enamel defects, and general alveolar bone loss.

Microcomputed Tomography (μCT) Scanning and Analysis

Each mandibular specimen was scanned and reconstructed at 18 × 18 × 18-μm voxels using a μCT system as previously described.[22] A three-dimensional volume viewer and analyzer software were used as the tool for three- and two-dimensional visualization and quantification. Linear bone loss was obtained by measuring the distance from the cementoenamel junction to the alveolar bone crest or to the base of the alveolar intrabony defect at the mesial surface of the mandibular second molar teeth. The measurements of coded specimens were made by two independent, calibrated examiners.

The Occlusal Hypofunction Model and Histologic Preparation

A model of occlusal hypofunction was developed to determine the in vivo effect of the lack of periostin on the periodontium's response to mechanical loading (occlusal function) and unloading (occlusal hypofunction).

To eliminate occlusal force on the right side, the mandibular incisors were trimmed weekly, using surgical clippers, to reduce the right incisor's edge starting at 10 days of age for 3 months. Six 10-day periostin-null mice per treatment group were used in this study.

The animals received water and regular diet freely after the procedure. At the end of the 3 months, the mice were sacrificed, and the dissected maxillary and mandibular specimens were immediately immersed in fixative (4% paraformaldehyde) overnight at 48°C. The tissues were decalcified with 19% EDTA solution[#] (pH 7.4) at 48°C for 3 weeks then dehydrated and embedded in paraffin. The tissue blocks were cut into 4-μm-thick mesio-distal serial sections and mounted on glass slides.

Immunohistochemistry

Immunostaining of periostin was performed on paraffin sections. Sections were incubated in blocking solution and goat serum for 15 minutes.[**] Primary affinity-purified anti-periostin antibody was diluted 1:6,000 in 0.1 M Tris (pH 7.6)/1% bovine serum albumin (BSA) for ≥1 hour. Slides were washed in 0.1 M Tris (pH 7.6)/1% Tween and incubated for ≥30 minutes with goat-rabbit-biotin-conjugated secondary antibody diluted 1:1,000 in 0.1 M Tris (pH 7.6)/1% BSA.[††] Slides were washed in 0.1 M Tris (pH 7.6)/1% Tween and incubated for 10 minutes with biotin tyramide amplification reagent[‡‡] and processed as described by the manufacturer. After diaminobenzidine staining, sections were counterstained with hematoxylin.

Cell Culture

For this study, we used a cell line known as PDL-L2, which has been found to mimic the gene expression of the PDL in vivo.[23] Briefly, this cell line was derived from molars from 5-week-old transgenic mice harboring the temperature-sensitive SV40 large T-antigen gene. Cells were placed in flexible gel substrate six-well tissue culture plates,[§§] coated with collagen type I

[¶]Model 8050-020, Field Emission, Willington, IL.
[#]Sigma-Aldrich, St. Louis, MO.
[**]Avidin/Biotin Block, Vector Laboratories, Burlingame, CA.
[††]Vector Laboratories.
[‡‡]Vectastain Elite ABC Kit, Vector Laboratories.

containing Dulbecco's modified Eagle's medium,[||||] supplemented with 10% fetal bovine serum, penicillin G (100 IU/ml), and streptomycin (100 mg/ml), and incubated at 33°C and 5% CO_2 in air.

Application of Tensional Force to the PDL Cells

A cyclic tensional force was applied to PDL cell cultures, using the cell culture–loading stations,[¶¶] by a procedure described by Banes et al.[24] Briefly, cells at passages three and four were cultured (1×10^5 cells/well) on flexible-bottomed culture plates for 48 hours until they became subconfluent. Fresh media were added every 24 hours until the application of the mechanical stress. To apply a tensile strain to the cells, the flexible bottoms of the plates were deformed to various extents by a computer-operated vacuum system. Cells were elongated (deformed) at six cycles/minute (i.e., 5 seconds on and 5 seconds off) and subjected to each of the three levels of strain (1%, 14%, and 20% increase in surface area of the bottom) for 48 hours. Non-stretched cells were used as controls.

RNA Isolation

Total RNA was isolated from cells at 0, 6, 24, 48, 56, 72, 96, and 120 hours after application of the mechanical strain. To isolate RNA from PDL-L2 cells, the cultures were washed twice with 2 ml each of PBS, and the RNA was extracted as instructed in the RNA extract kit[##] used. The RNA was treated with 27 units of DNase.[***]

Quantitative Real-Time PCR

A two-step real-time PCR protocol was used.[†††] RNA was first converted to cDNA at 37°C for 2 hours.[‡‡‡] The real-time PCRs were performed on a DNA sequence detector,[§§§] using 20 ng cDNA per reaction. The conditions for PCR were as follows: 2 minutes at 50°C and 10 minutes at 95°C; then, 40 cycles each of 15 seconds at 95°C and 1 minute at 60°C on optical 96-well plates;[||||||] and covered with optical caps. Each plate contained triplicates of the test cDNA templates and no-template controls for each reaction mix. The expression for each mouse gene was normalized to murine GAPDH.

Statistical Analysis

The significance of differences between mean values of experimental and control groups were determined by one-way analysis of variance. A P value <0.05 was considered significant.

Results

Tissue and Cellular Defects Within the PDL in Periostin-Null Mice

Within the periodontium, the PDL fibroblasts, not the cementoblasts or the osteoblasts, were the cells that expressed periostin (Fig. 1). Once the molecule was secreted, it was distributed within the extracellular PDL space (Fig. 2A). When adult normal periodontium was compared to that of periostin-null mice, the differences were dramatic (Figs. 2B and 2C). The periodontium deteriorates with time. It is characterized by severe alveolar bone loss along with

[§§]Bio-Flex 6-well tissue culture plates, Flexcell International, Hillsborough, NC.
[||||]Gibco BRL, Invitrogen, Carlsbad, CA.
[¶¶]Bio-Flex loading stations, Flexcell International.
[##]QIAshredder and RNeasy, Qiagen, Valencia, CA.
[***]DNase I, Qiagen.
[†††]Taqman, Applied Biosystems, Foster City, CA.
[‡‡‡]High Capacity cDNA Archive kit, Applied Biosystems.
[§§§]ABI Prism 7700, Applied Biosystems.
[||||||]MicroAmp Optical 96-well plates, Applied Biosystems.

attachment loss, external root resorption and widening of the PDL. However, before tooth eruption, no defects were observed in the periostin-null mouse (Figs. 2D and 2E). Once the teeth erupted and started sustaining the occlusal load, the lack of periodontal integrity became obvious in the null mice and lead to alveolar bone defects and malformed incisors (Figs. 2F and 2G).

In contrast to the normal mice, the periodontal defects in the periostin-null mice worsened over time (Figs. 3A and 3B). The dramatic loss of periodontal support often resulted in premature tooth loss or pathologic migration, particularly of the third molar. The three-dimensional characteristics of some of these defects can be clearly observed in the μCT images (Figs. 3C and 3D). Linear quantitation of the alveolar defects clearly demonstrated a significant difference compared to normal control mice (Fig. 4).

Within the PDL space of the incisors, rodents have a force-resistant, cylindrical, single-layer epithelium of ameloblastic cells that is responsible for the formation of enamel found on the incisor's facial surface. The integrity of this layer remained undisturbed even under the mechanically challenging environment that developed after the incisors fully erupted. In the periostin-null mice, the ameloblast layer maintained its integrity while the incisors were unerupted, and the enamel layer developed normally. However, after eruption, the integrity of the enamel layer in the periostin-null mice was compromised, and a deformed, irregular enamel layer formed (Figs. 5A and 5B).

Cementoblasts are another type of cells found within the PDL; they are responsible for the formation of cementum. Cementoblasts are recruited to the root surface and attach to it, engaging the PDL fibers to the tooth (Figs. 5C and 5E). In the periostin-null mice, the cementoblasts failed to attach to the root surface, thereby compromising the attachment apparatus (Figs. 5D and 5F).

Tooth Unloading Model for the Removal of Occlusal Force

Figure 6A illustrates the reduced mandibular incisors, and Figure 6B shows the intact side in the same mouse. The right mandibular incisor was reduced weekly, whereas the tooth on the left side was allowed to erupt normally and sustain normal occlusal loads. The results were striking; in the absence of a mechanically challenging environment, no enamel or periodontal defect developed (Fig. 6A). However, the opposing incisor presented the defects because it continued to sustain indirect load from the contralateral mandibular incisor (Fig. 6B). Histologically, the ameloblast's morphology remained relatively intact in the absence of load (Fig. 7A), whereas the loaded side developed the characteristic defects (Figs. 7B and 7D). However, regularly spaced small defects are still seen in the enamel layer of the reduced side and might have resulted from the weekly reduction of the incisors (Figs. 7A and 7C). The characteristic widening of the PDL space in the periostin-null erupted teeth was almost entirely corrected by decreasing the mechanical stress to this tissue (Fig. 8). Linear quantitation of the periodontal defect in the periostin-null mice showed ~50% PDL width reduction when measured from the alveolar bone to the root cementum. In addition, it can clearly be seen that the cementoblasts were recruited and able to attach to the root surface in the periostin-null reduced incisor (Fig. 8C).

TGF-β Was Responsible for Increased Expression of Periostin in Response to Mechanical Loading of PDL Cells In Vitro

PDL cells were exposed to various magnitudes of tensile strain for 0, 6, 24, 48, 56, 72, 96, and 120 hours and subsequently analyzed for periostin mRNA expression (Fig. 9). Real-time PCR analysis revealed a time-dependent increase in periostin occurring in the 14% strain group (Fig. 9A), reaching a 3.2-fold increase after 24 hours followed by a greater increase at 48 hours.

After cessation of the stretching regimen, periostin mRNA levels rapidly decreased to levels of expression similar to those found in the control group, remaining stable over time. The expression of periostin mRNA in the 1% strain group did not show any significant changes over the 48-hour regimen of substrate strain (data not shown). A baseline level of periostin seemed to be maintained, even in the absence of load. Because TGF-β was shown to be regulated by loading and to regulate periostin expression,[14,21] we examined TGF-β expression and used neutralizing antibody to this growth factor. Like periostin, TGF-β mRNA was also upregulated under the same stretching regimen. The TGF-β response preceded that of the periostin gene where maximal expression was observed at 12 hours for TGF-β and at 48 hours for periostin (Fig. 9B). The potential regulation of periostin by TGF-β was tested by incubating the PDL cells with TGF-β1 neutralizing antibodies; the periostin response was blocked completely (Fig. 9C).

Discussion

The present study was designed to determine the role of periostin in the PDL to maintain function during mechanical loading. Knowing the detrimental effect of functional load in the absence of periostin, we investigated the effect of hypofunction in the periodontium of periostin-null mice. We hypothesized that periostin is regulated by mechanical load and that its functional importance is diminished under conditions of occlusal hypofunction. Although several methods were used in previous studies[19,25] to create experimental periodontal hypofunction, mechanical occlusal reduction was chosen to produce occlusal hypofunction in our studies. We found this method to be the least invasive and most reproducible to achieve hypofunction. In addition, unlike the soft diet method, this method allowed us to use the contralateral side as a corresponding control.

By clipping one of the incisors, the mechanical stimulus that is detrimental to the PDL as well to the ameloblast layer in the periostin-null mouse was significantly reduced. As in the case of unerupted teeth, no significant mechanical challenge was transferred from the tooth to the periodontium. The non-clipped side developed the characteristic pseudostratified ameloblast layer favoring the formation of cyst-like structures. In contrast, similar to the wild type or the unerupted incisors on the reduced loading side, the ameloblast layer maintained its integrity and was able to form a fairly normal enamel surface. Regularly spaced small defects were detected along the epithelial layer and the unmineralized enamel surface on the clipped side. These small defects were transient and did not compromise the overall integrity of the enamel-producing organ. Its pattern of appearance led to the conclusion that these defects were caused by the mechanical loading of the tooth during the clipping process. The ameloblast morphology recovered between these defects at regular intervals, lending support to this hypothesis. These transient stimuli were transferred and, in the absence of periostin, were clearly strong enough to elicit reversible loss of integrity and compromised attachment of the ameloblasts in the epithelial layer.

Periostin expression was shown to increase in areas of compression and decrease in areas of tension in the tooth-movement model.[18] In the periostin-null mouse, severe periodontal defects develop after the teeth erupt and begin to sustain occlusal loads.[12] These findings suggest a mechanical feedback regulatory mechanism of gene expression important for periodontal integrity.

Several interactions between cells and a diverse mixture of matrix proteins take place within this very narrow, yet precisely regulated, space. Particularly interesting is the exclusive expression of periostin by PDL cells. Within the periodontium, periostin is highly expressed and specifically present in the PDL, and its expression increases in the adult fully erupted

dentition.[26] In addition, it was reported that orthodontic force induced divergent changes of periostin mRNA expression between the compression and tension sites of the PDL.[18]

After teeth erupt in the periostin-null mouse, the periodontium deteriorates with time, and severe alveolar bone loss, attachment loss, external root resorption, and widening of the PDL clearly develop within a highly inflamed background.[12] This compromised integrity of the periodontium found in the adult periostin-null mice contrasted with an entirely normal-appearing and structurally stable periodontium found in the control mice. However, these detrimental changes to the tooth-supporting tissues were not evident prior to tooth eruption.

The use of the murine animal model provided additional evidence that periostin is an important molecule in the attachment and integrity of the various cells within the PDL space. Within the PDL space of incisors, rodents possess a force-resistant, cylindrical, single-layer epithelium of ameloblasts cells that is responsible for the formation of the enamel found on their incisor's facial surface. The integrity of this layer remains undisturbed, even in the mechanically challenging environment that develops after the incisors fully erupt. In the periostin-null mice, the ameloblast layer maintained its integrity prior to incisor eruption coincident with normal enamel layer development. However, after eruption, the integrity of the periostin-null enamel layer was compromised, and a deformed, irregular enamel layer formed.

PDL and alveolar bone cells are exposed to physical forces in vivo after the teeth completely erupt. The PDL may be the medium of force transfer and the means by which alveolar bone remodels in response to applied forces. Therefore, it is important to understand and explore the factors that contribute to the biophysical attributes of the PDL. In this study, we tested the in vitro ability of PDL fibroblasts to respond to mechanical strain to regulate periostin expression and, therefore, regulate its availability during normal occlusal function. A wide range of approaches to model external force application in vitro have been used. These include subjecting cells to shear stress, hydrostatic pressure, and strain of deformable substrates.[27] Substrate stretching represents a validated method for tensional force that closely mimics the strain to which the PDL is subjected during mastication or tooth movement. We found an increase in periostin expression during loading that decreased upon cessation of loading. We also found an increase in message for TGF-β, a multifunctional cytokine shown to be a potent inducer of matrix protein expression[20] and of periostin.[14] The use of neutralizing antibody to the TGF-β1 isoform completely blocked the effects of loading on periostin expression. These data suggest that mechanical loading most likely activates TGF-β1 from its latent complex, which, in turn, stimulates periostin production.

Conclusions

The periostin response to mechanical loading was controlled by TGF-β in PDL fibroblasts, potentially through the activation of latent TGF-β. Collectively, the in vivo and in vitro data highlight the functional importance of periostin in maintaining the structural integrity of the periodontium during occlusal function.

Acknowledgements

The authors thank Dr. Hiroyuki Kawashima, Divisions of Cell Biology and Molecular Pharmacology, Niigata University Graduate School of Medical and Dental Sciences, Niigata, Japan, for providing the PDL-L2 cell lines, as well as the National Institutes of Health (National Institutes of Health/National Institute of Dental and Craniofacial Research [NIH/NIDCR]), Bethesda, Maryland, for providing the funds necessary for this study (NIH/NIDCR T32 DE 07294, DE 13480, and DE 13397).

References

1. McCulloch CA, Lekic P, McKee MD. Role of physical forces in regulating the form and function of the periodontal ligament. Periodontol 2000 2000;24:56–72. [PubMed: 11276873]
2. Arora PD, McCulloch CA. Dependence of collagen remodelling on alpha-smooth muscle actin expression by fibroblasts. J Cell Physiol 1994;159:161–175. [PubMed: 8138584]
3. Jones DB, Nolte H, Scholübbers JG, Turner E, Veltel D. Biochemical signal transduction of mechanical strain in osteoblast-like cells. Biomaterials 1991;12:101–110. [PubMed: 1652292]
4. Cohn SA. Disuse atrophy of the periodontium in mice following partial loss of function. Arch Oral Biol 1966;11:95–105. [PubMed: 5226737]
5. Deporter DA, Svoboda EL, Motruk W, Howley TP. A stereologic analysis of collagen phagocytosis by periodontal ligament fibroblasts during occlusal hypofunction in the rat. Arch Oral Biol 1982;27:1021–1025. [PubMed: 6963882]
6. Doi T, Ohno S, Tanimoto K, et al. Mechanical stimuli enhances the expression of RGD-CAP/betaig-h3 in the periodontal ligament. Arch Oral Biol 2003;48:573–579. [PubMed: 12828986]
7. Levy GG, Mailland ML. Histologic study of the effects of occlusal hypofunction following antagonist tooth extraction in the rat. J Periodontol 1980;51:393–399. [PubMed: 6930479]
8. Pihlstrom BL, Ramfjord SP. Periodontal effect of non-function in monkeys. J Periodontol 1971;42:748–756. [PubMed: 5000895]
9. Tanaka E, Inubushi T, Nullolstra JH, et al. Comparison of dynamic shear properties of the porcine molar and incisor periodontal ligament. Ann Biomed Eng 2006;34:1917–1923. [PubMed: 17063388]
10. Watarai H, Warita H, Soma K. Effect of nitric oxide on the recovery of the hypofunctional periodontal ligament. J Dent Res 2004;83:338–342. [PubMed: 15044510]
11. Youn SH, Maeda T, Kurisu K, Wakisaka S. Alteration in the expression level of calbindin D28k in the periodontal ligament of the rat molar during experimental tooth movement. Arch Histol Cytol 1999;62:139–147. [PubMed: 10399538]
12. Rios H, Nullushik SV, Wang H, et al. Periostin null mice exhibit dwarfism, incisor enamel defects, and an early-onset periodontal disease-like phenotype. Mol Cell Biol 2005;25:11131–11144. [PubMed: 16314533]
13. Takeshita S, Kikuno R, Tezuka K, Amann E. Osteoblast-specific factor 2: Cloning of a putative bone adhesion protein with homology with the insect protein fasciclin I. Biochem J 1993;294:271–278. [PubMed: 8363580]
14. Horiuchi K, Amizuka N, Takeshita S, et al. Identification and characterization of a novel protein, periostin, with restricted expression to periosteum and periodontal ligament and increased expression by transforming growth factor beta. J Bone Miner Res 1999;14:1239–1249. [PubMed: 10404027]
15. Gillan L, Matei D, Fishman DA, Gerbin CS, Karlan BY, Chang DD. Periostin secreted by epithelial ovarian carcinoma is a ligand for alpha(V)beta(3) and alpha(V)beta(5) integrins and promotes cell motility. Cancer Res 2002;62:5358–5364. [PubMed: 12235007]
16. Bao S, Ouyang G, Bai X, et al. Periostin potently promotes metastatic growth of colon cancer by augmenting cell survival via the Akt/PKB pathway. Cancer Cell 2004;5:329–339. [PubMed: 15093540]
17. Norris RA, Damon B, Mironov V, et al. Periostin regulates collagen fibrillogenesis and the biomechanical properties of connective tissues. J Cell Biochem 2007;101:695–711. [PubMed: 17226767]
18. Wilde J, Yokozeki M, Terai K, Kudo A, Moriyama K. The divergent expression of periostin mRNA in the periodontal ligament during experimental tooth movement. Cell Tissue Res 2003;312:345–351. [PubMed: 12761672]
19. Afanador E, Yokozeki M, Oba Y, et al. Messenger RNA expression of periostin and Twist transiently decrease by occlusal hypofunction in mouse periodontal ligament. Arch Oral Biol 2005;50:1023–1031. [PubMed: 15922993]
20. Bonewald, LF. Transforming growth factor beta. In: Bilezikian, JP.; Raisz, LG.; Rodan, GA., editors. Principles of Bone Biology. San Diego, CA: Academic Press; 2002. p. 903-918.

21. Hori Y, Katoh T, Hirakata M, et al. Anti-latent TGF-beta binding protein-1 antibody or synthetic oligopeptides inhibit extracellular matrix expression induced by stretch in cultured rat mesangial cells. Kidney Int 1998;53:1616–1625. [PubMed: 9607192]

22. Park CH, Abramson ZR, Taba M Jr, et al. Three-dimensional micro-computed tomographic imaging of alveolar bone in experimental bone loss or repair. J Periodontol 2007;78:273–281. [PubMed: 17274716]

23. Saito Y, Yoshizawa T, Takizawa F, et al. A cell line with characteristics of the periodontal ligament fibroblasts is negatively regulated for mineralization and Runx2/Cbfa1/Osf2 activity, part of which can be overcome by bone morphogenetic protein-2. J Cell Sci 2002;115:4191–4200. [PubMed: 12356921]

24. Banes AJ, Link GW Jr, Gilbert JW, Tran Son Tay R, Monbureau O. Culturing cells in a mechanically active environment. Am Biotechnol Lab 1990;8:12–22. [PubMed: 1366543]

25. Carranza FA Jr, Cabrini RL, Lopez Otero R, Stahl SS. Histometric analysis of interradicular bone in protein deficient animals. J Periodontal Res 1969;4:292–295. [PubMed: 4244937]

26. Kruzynska-Frejtag A, Wang J, Maeda M, et al. Periostin is expressed within the developing teeth at the sites of epithelial-mesenchymal interaction. Dev Dyn 2004;229:857–868. [PubMed: 15042709]

27. Norton LA, Andersen KL, Arenholt-Bindslev D, Andersen L, Melsen B. A methodical study of shape changes in human oral cells perturbed by a simulated orthodontic strain in vitro. Arch Oral Biol 1995;40:863–872. [PubMed: 8651891]

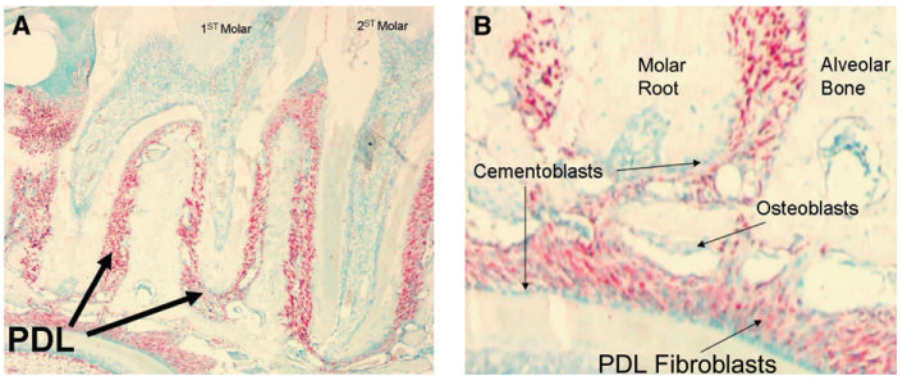

Figure 1.

Periostin mRNA expressed by PDL fibroblasts. Periostin in situ hybridization showing its localization to PDL fibroblasts within the dental alveolar area **(A)**. Note that the in situ hybridization signal (red color) is contained within the PDL spaces. **B)** Higher-magnification image clearly depicting the periostin message within the PDL fibroblasts but not in the osteoblasts or the cementoblasts. (Original magnification: A, ×4; B, ×20.)

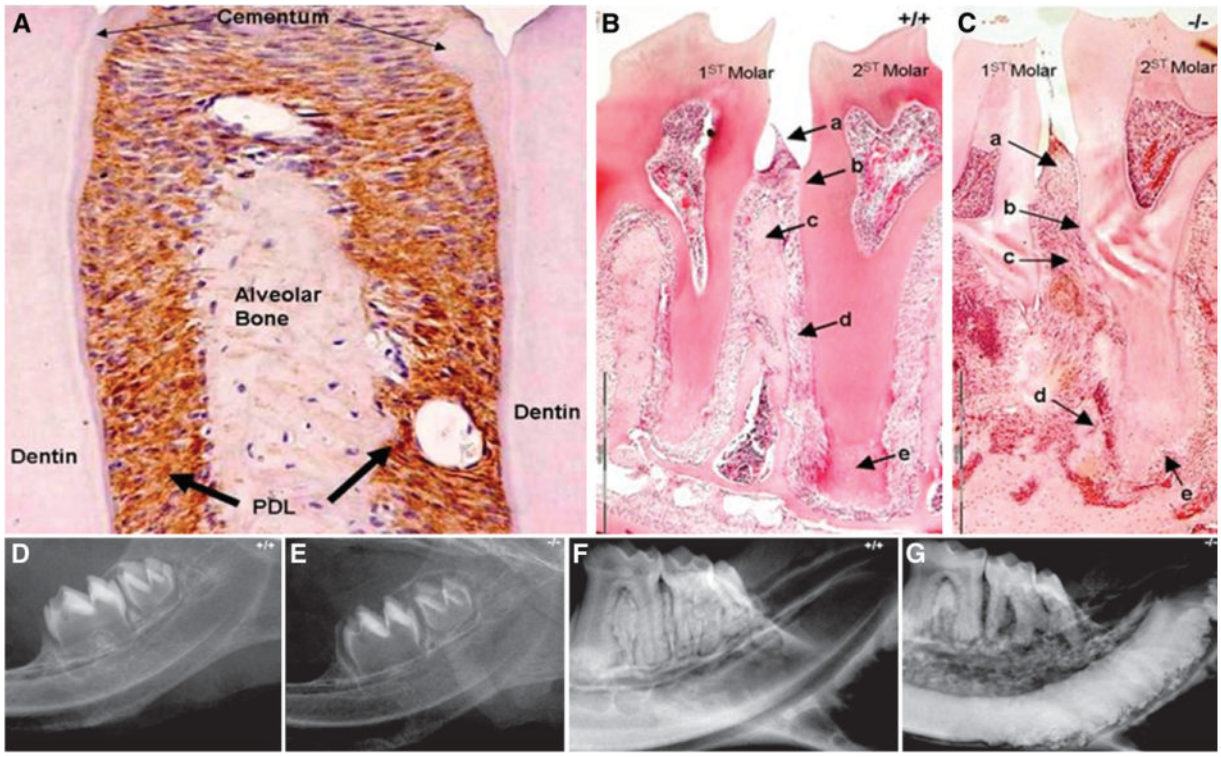

Figure 2.

Loss of periostin results in dramatic periodontal defects. **A)** Within the periodontal attachment apparatus, periostin localizes exclusively within the PDL as shown here by immunostaining (brown color). **B)** With normal periostin expression, as in the wild-type control mice, the periodontium can be described by a well-defined (a) gingival tissue, (b) cervical epithelial attachment, (c) intact crestal alveolar bone, (d) narrow and regular PDL thickness, and (e) appropriate thickness of root cementum. **C)** In the absence of periostin (periostin-null mice), several defects become evident after the tooth eruption. The null periodontium displays (a) enlarged gingival tissue, (b) attachment loss, (c) irregular PDL, (d) dramatic alveolar bone loss, and (e) external root resorption. **D and E)** The periodontium of the null and wild-type animals appears intact when the teeth are unerupted. **F)** The wild-type adults maintain an intact and functional periodontium. **G)** The adult null animal develops rapid alveolar bone loss and obvious enamel defects affecting the incisors. (Original magnification: A, ×20; B and C, ×4.)

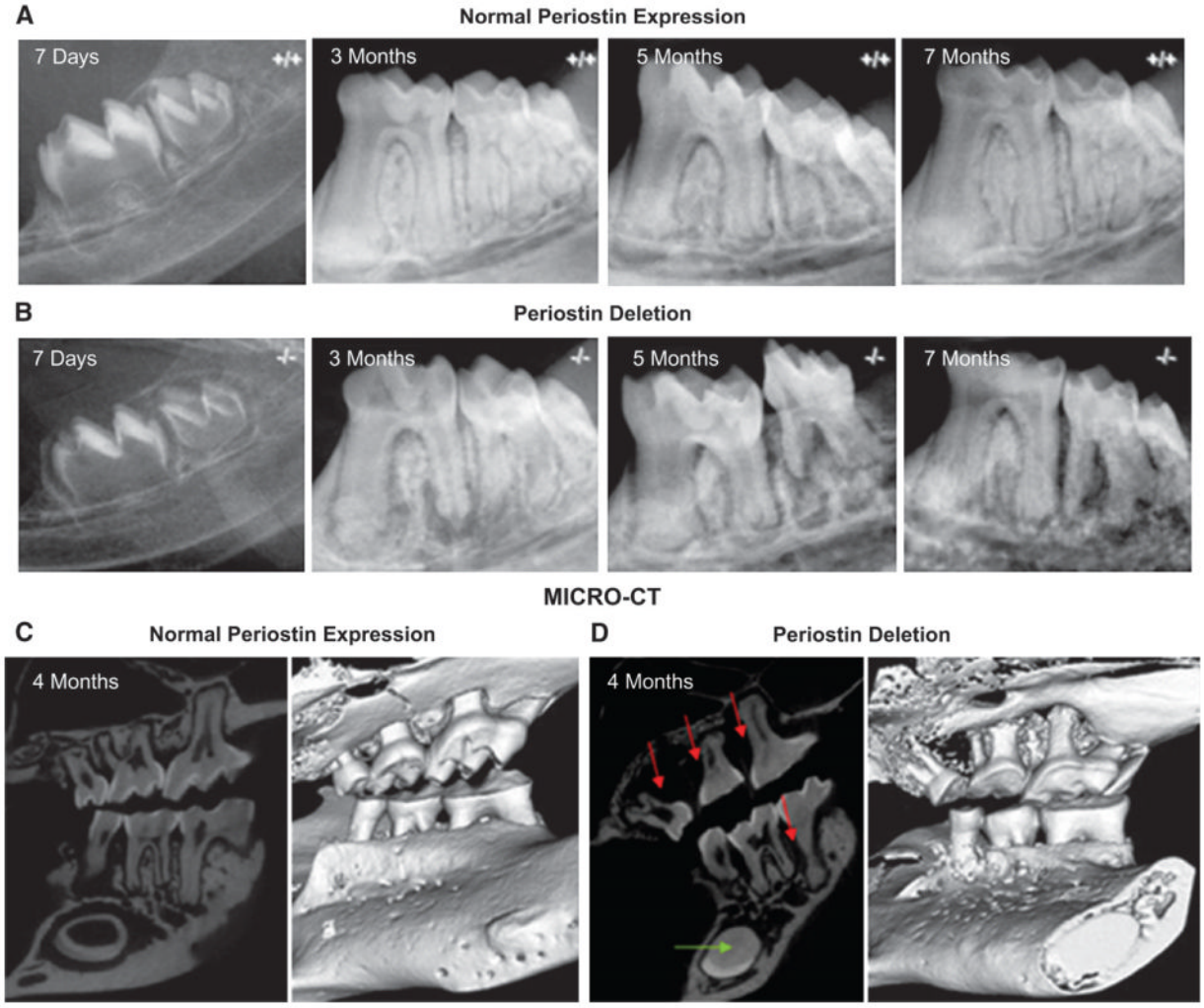

Figure 3.

Periodontal defects worsened with age in the periostin-null mouse. **A)** Normal periodontal development and homeostasis in the control mouse. **B)** In the periostin-null mouse, molar teeth develop normally as reflected in the 7-day image. However, significant periodontal changes occur after the teeth erupt and start to sustain a normal occlusal load. The periodontal abnormalities can be detected radiographically at 3, 5, and 7 months, demonstrating a tendency to worsen with age. **C and D)** Micro-CT visualization of the periodontal tissues confirms the presence, extent, and severity of these defects (red arrows) and clearly accentuates the dramatic periodontal difference that results from a complete lack of periostin expression. In addition, notice the complete obliteration of the incisor pulp chamber (green arrow).

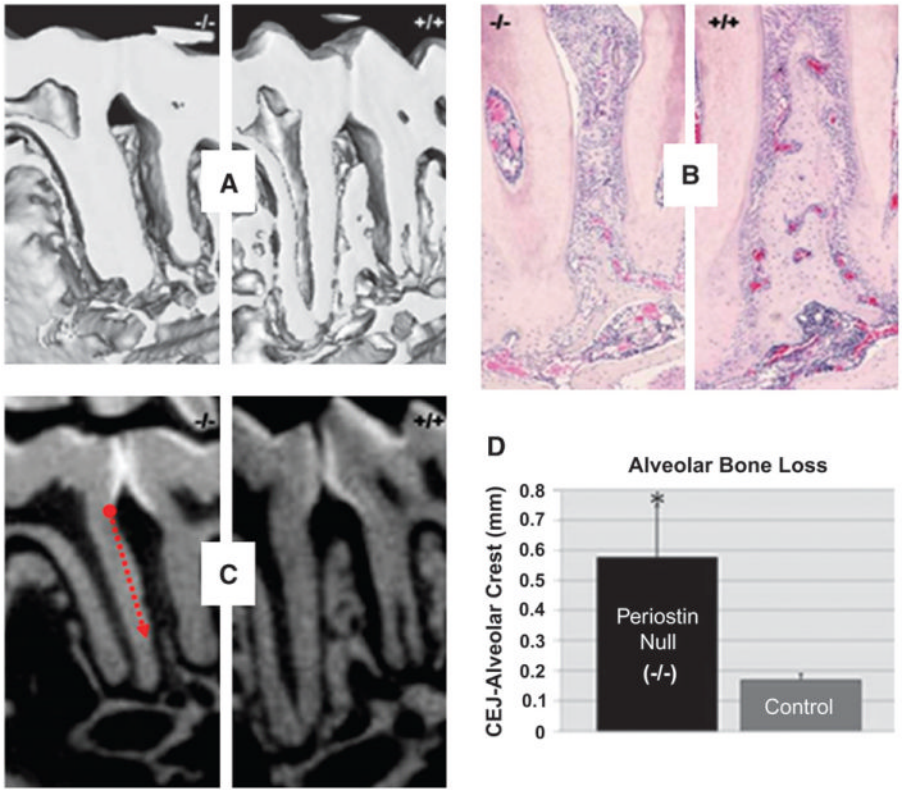

Figure 4.

Alveolar bone loss is significantly greater in the periostin-null mice compared to control mice. **A)** Micro-CT qualitative assessment of interradicular alveolar bone defects. **B)** Histology confirms the altered integrity of the periodontal structures (hematoxylin and eosin; original magnification, ×4.) **C and D)** Linear quantitation of the interproximal alveolar bone from the cemento-enamel junction (CEJ) to the most coronal aspect of the alveolar crest reflects significant differences in the absence of periostin protein. **P* <0.05.

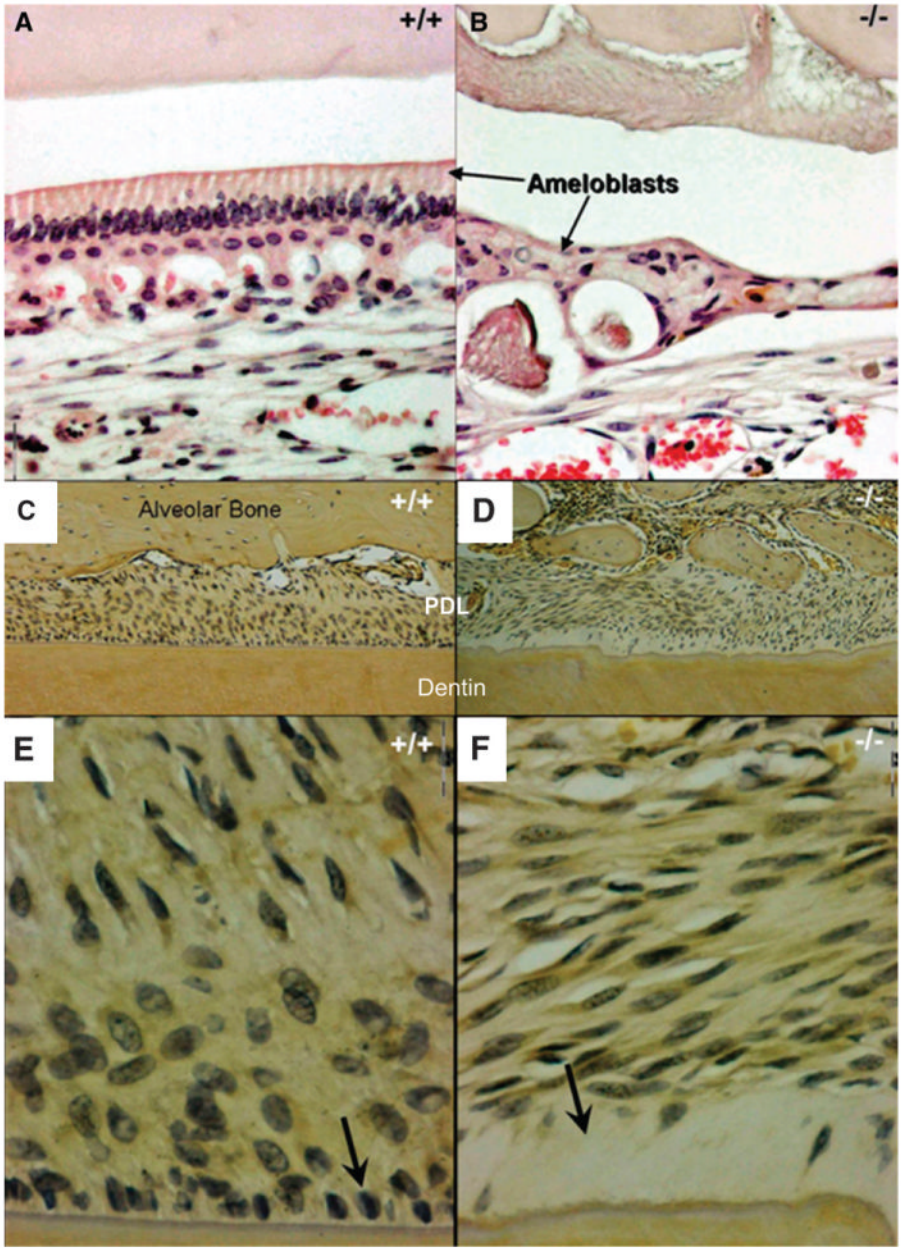

Figure 5.

Cyst formation in the ameloblast layer and detached cementoblasts in the periostin-null peridontium. **A)** The wild-type adult mice present a well-organized ameloblast layer composed of polarized cylindrical simple epithelium. **B)** The periostin knock-out mice display a disorganized pseudostratified epithelial layer that is poorly attached and appears to produce an amorphous matrix that covers the dentin and that is also present ectopically within this matrix-producing organ. **C and E)** Normal attachment and distribution of cementoblasts at the root surface (arrow) in the wild-type control. **D and F)** Periostin-null periodontium. Notice the absence of cementoblasts and an apparent disengagement of the PDL from the root surface. Note the absence of cementoblasts attached to the root surface (arrow). (H&E staining: A and B; TRAP and hematoxylin staining: C, D, E, and F; original magnification: A and B, ×20; C and D, ×10; E and F, ×40.)

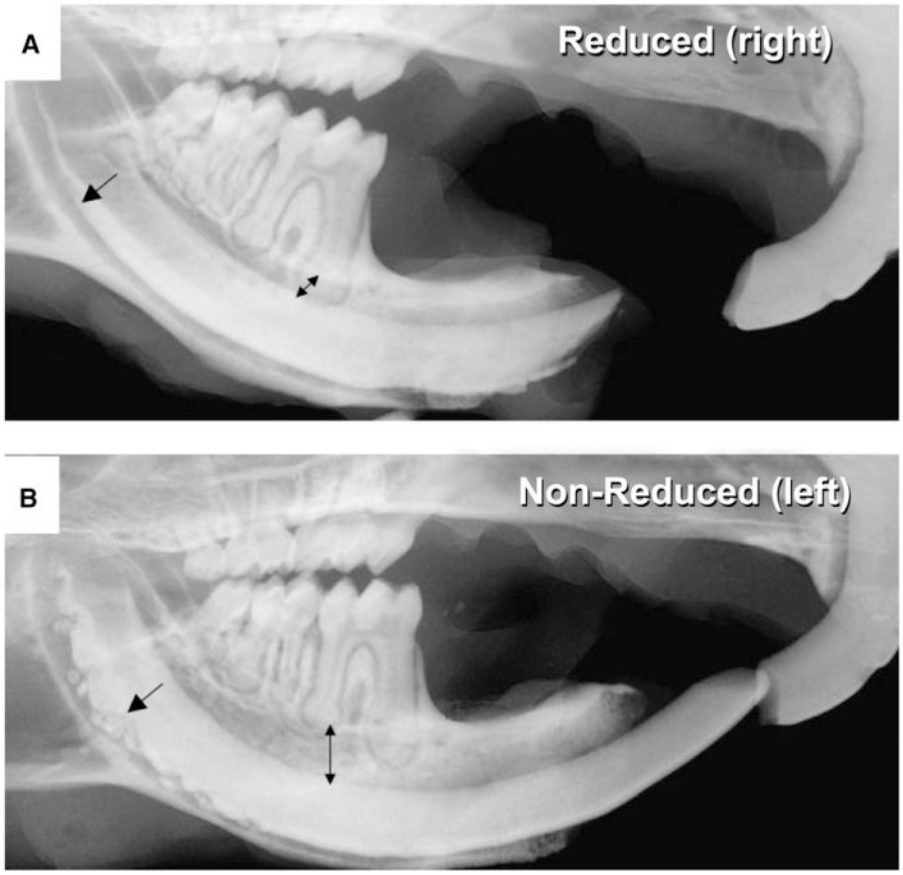

Figure 6.

Incisal reduction of the lower incisor rescues the phenotype. **A)** The hypofunction condition was created by taking one mandibular incisor of the periostin-null mice out of occlusion by trimming the incisal edge weekly for 3 months starting at 10 days. **B)** The contralateral incisor was left intact to be used as an internal control. Arrows denote normal anatomy in A and altered anatomy in B.

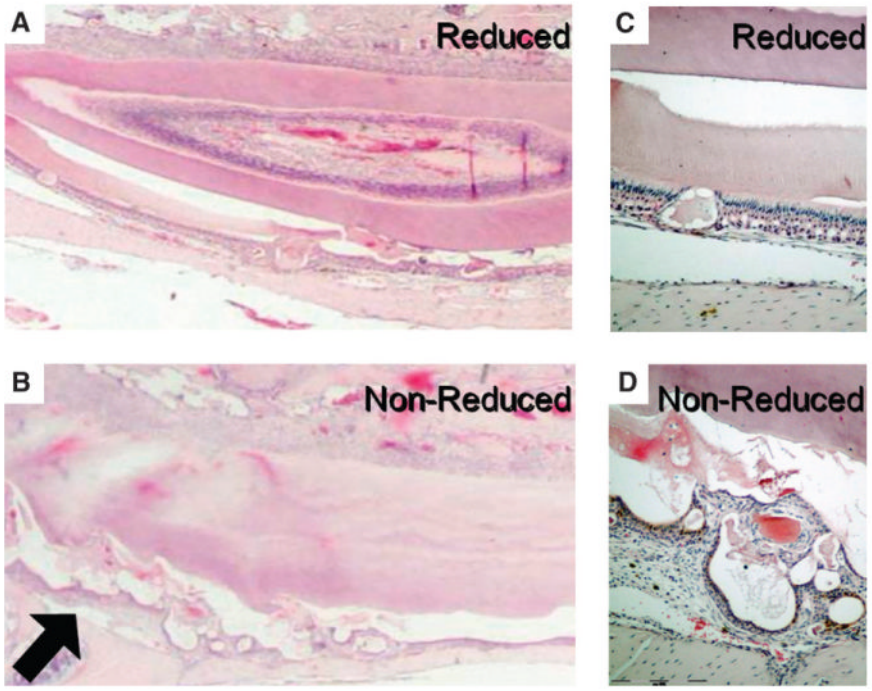

Figure 7.

Partial rescue of the ameloblast layer by removal of occlusal force. **A)** Trimmed incisor from the knock-out mouse. Note the fairly homogeneous enamel surface as well as the ameloblast layer. **B)** The untrimmed side showing increased cyst formation (arrow). **C)** Higher magnification of the ameloblast layer on the trimmed side showing one of the small defects. **D)** Higher magnification of the irregular and detached ameloblast layer on the untrimmed side. (H&E staining: A through D; original magnification: A and B, ×1; C and D, ×10).

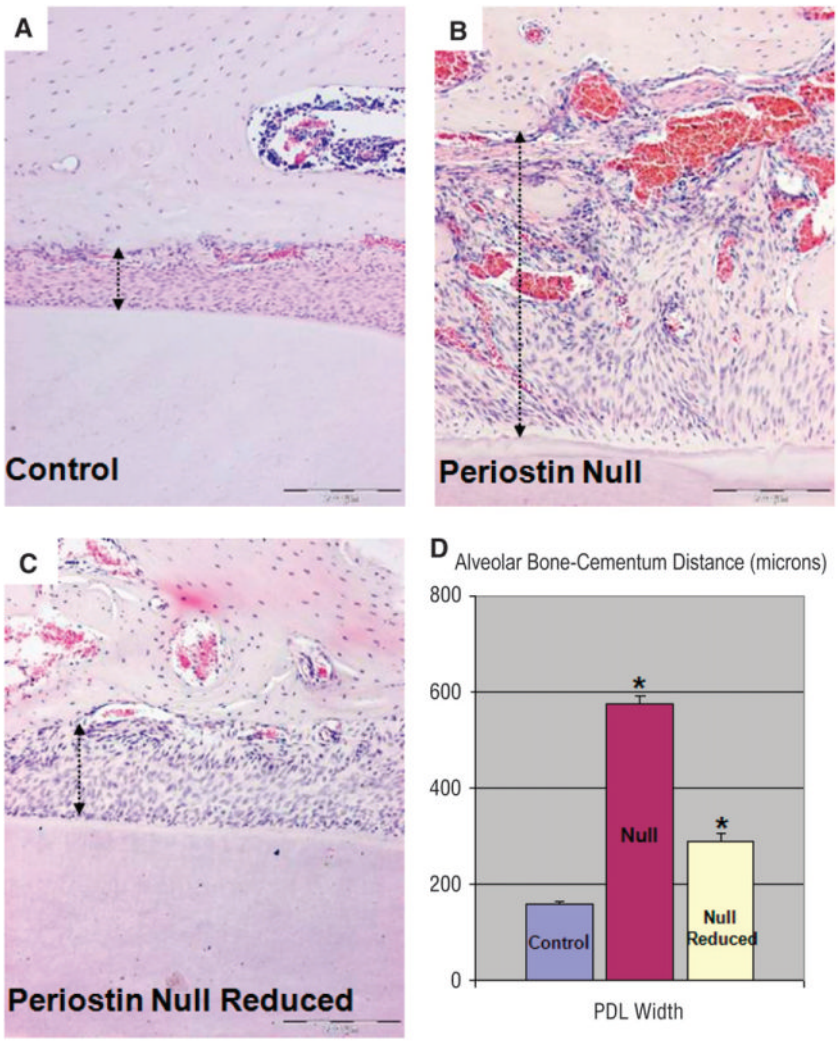

Figure 8.

Partial rescue of the PDL by removal of occlusal force. **A)** Wild-type PDL space: alveolar wall is intact and the root surface is covered by attached cementoblasts. In addition, the PDL fibers are well organized. **B)** Null PDL: untrimmed side. The alveolar wall is irregular and discontinuous, there is lack of attachment of cementoblasts to the root surface, the PDL space is widened, and the PDL fibers lack organization. **C)** Null PDL: trimmed side. Histologically, the PDL width has decreased close to that of the wild-type mouse, the orientation of the fibers appears mildly affected, and the adjacent alveolar bone wall recovers its continuity. **D)** PDL width calculated in microns from comparable areas in all three groups (*P <0.05). (Original magnification: A through C, ×10.) Arrows depict PDL width.

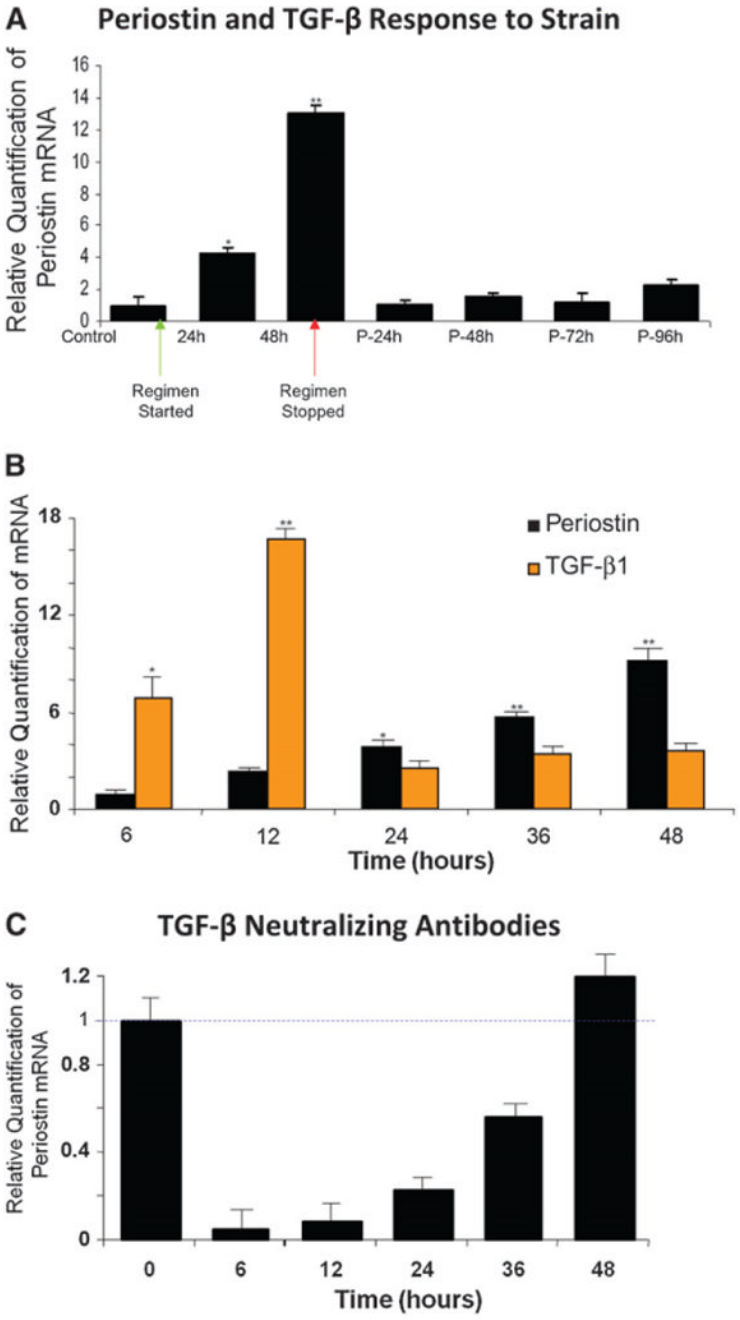

Figure 9.

Mechanical strain modulates periostin mRNA expression in PDL fibroblasts through TGF-β1. **A)** Time course variation of periostin mRNA levels following 14% stretching regimen. Periostin mRNA increased by 3.8 and 9.2-fold at 24 and 48 hours (h), respectively. The letter P = unloaded culture time points. **B)** Changes in TGF-β mRNA levels are ahead of that of periostin after mechanical stretching. TGF-β mRNA increased by 6.9-, 16.7-, 2.5-, 3.4-, and 3.6-fold at 6, 12, 24, 36, and 48 hours, respectively. **C)** Neutralizing TGF-β antibody (2.5 μg/ml) sharply reduced periostin response to mechanical stretching in PDL cells. **P* <0.05; ***P* <0.005.